Supporting Information

Photocatalytic Oxygenation of Substrates by Dioxygen with Protonated Manganese(III) Corrolazine

Jieun Jung,[†] Heather M. Neu,[‡] Pannee Leeladee,[‡] Maxime A. Siegler,[‡] Kei Ohkubo,[§] David P. Goldberg,[‡] and Shunichi Fukuzumi*[†,§,||]*

[†]*Department of Chemistry and Nano Science, Ewha Womans University, Seoul 120-750, Korea*

[‡]*Department of Chemistry, The Johns Hopkins University, 3400 North Charles Street, Baltimore, Maryland 21218, United States*

[§]*Department of Material and Life Science, Graduate School of Engineering, Osaka University, ALCA and SENTAN, Japan Science and Technology Agency (JST), Suita, Osaka 565-0871, Japan*

[||]*Faculty of Science and Engineering, Meijo University, ALCA and SENTAN, Japan Science and Technology Agency (JST), Nagoya, Aichi 468-0073, Japan*

E-mail: fukuzumi@chem.eng.osaka-u.ac.jp, dpg@jhu.edu

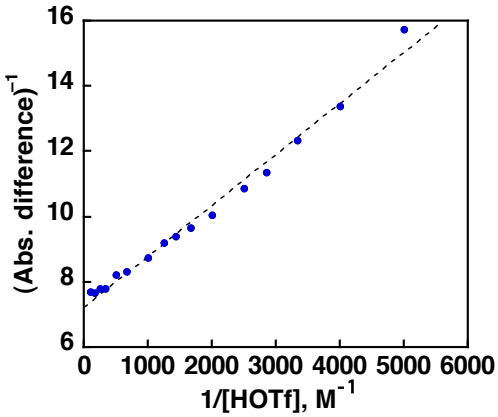

Figure S1. Plot of $(\Delta\text{Abs.})^{-1}$ vs $[\text{HOTf}]^{-1}$ to determine the second binding constant (K_2 = $[[\text{Mn}^{\text{III}}(\text{OTf})(\text{H}_2\text{O})(\text{TBP}_8\text{Cz(H)}_2)][\text{OTf}]]/[\text{Mn}^{\text{III}}(\text{OTf})(\text{TBP}_8\text{Cz(H)})][\text{H}^+]$) upon addition of HOTf ($0.0 - 1.0 \times 10^{-2}$ M) into the solution of $\text{Mn}^{\text{III}}(\text{OTf})(\text{TBP}_8\text{Cz(H)})$ (1.0×10^{-5} M) in PhCN.

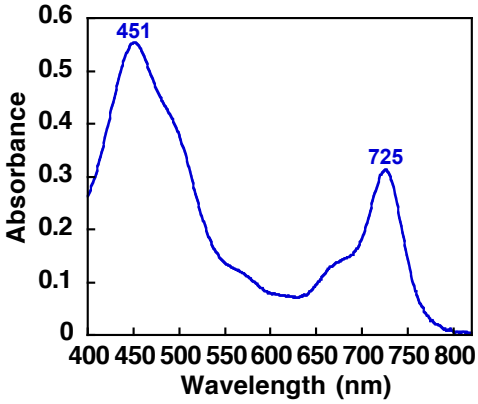

Figure S2. (a) UV–vis spectrum of crystalline [Mn^{III}(OTf)(TBP_8Cz(H))] dissolved in PhCN (2.0 mL) at 23 °C.

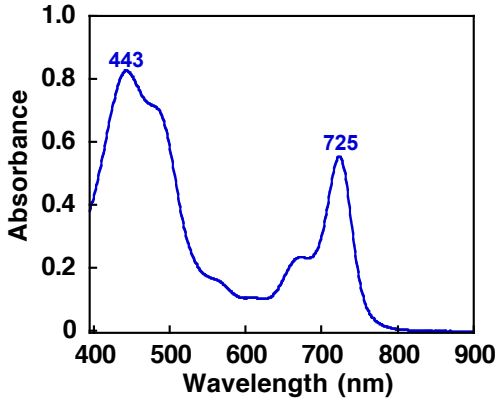

Figure S3. (a) UV–vis spectrum of crystalline [Mn^{III}(OTf)(TBP_8Cz(H))] dissolved in CH_2Cl_2 (2.0 mL) at 23 °C.

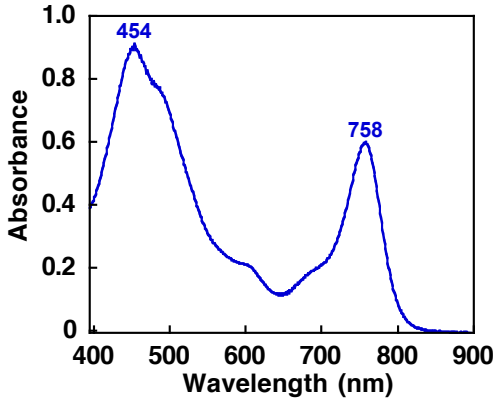

Figure S4. (a) UV–vis spectrum of crystalline $[Mn^{III}(OTf)(H_2O)(TBP_8Cz(H)_2)][OTf]$ dissolved in CH_2Cl_2 (2.0 mL) at 23 °C.

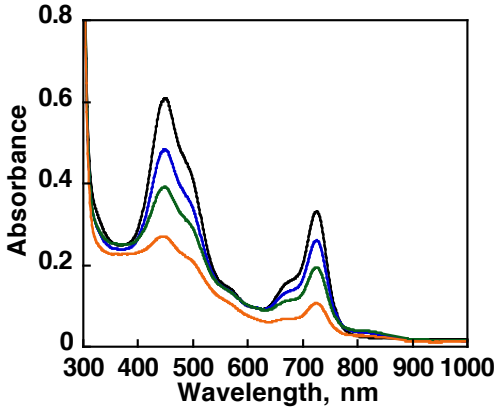

Figure S5. UV–vis spectral change of $Mn^{III}(OTf)(TBP_8Cz(H))$ (1.0×10^{-5} M) during photocatalytic oxidation reaction [black: 0 h, blue: 2 h, green: 4 h, and orange: 6 h] of HMB (0.3 M) in the presence of 4.0×10^{-5} M of HOTf under photoirradiation (white light) in an O_2–saturated PhCN solution at room temperature.

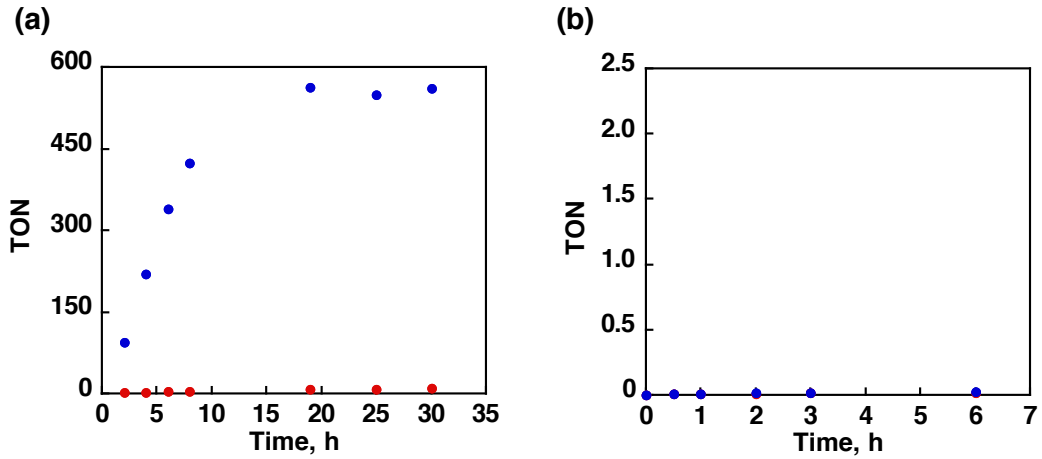

Figure S6. Time profiles of the amount of produced pentamethylbenzyl alcohol for photocatalytic oxidation reaction of HMB (0.3 M) by $(TBP_8Cz)Mn^{III}$ (1.0×10^{-5} M) (a) in the presence of 4.0×10^{-5} M of HOTf or (b) in the presence of 5.0×10^{-3} M of HOTf under photoirradiation (white light) in an O_2–saturated PhCN solution at room temperature.

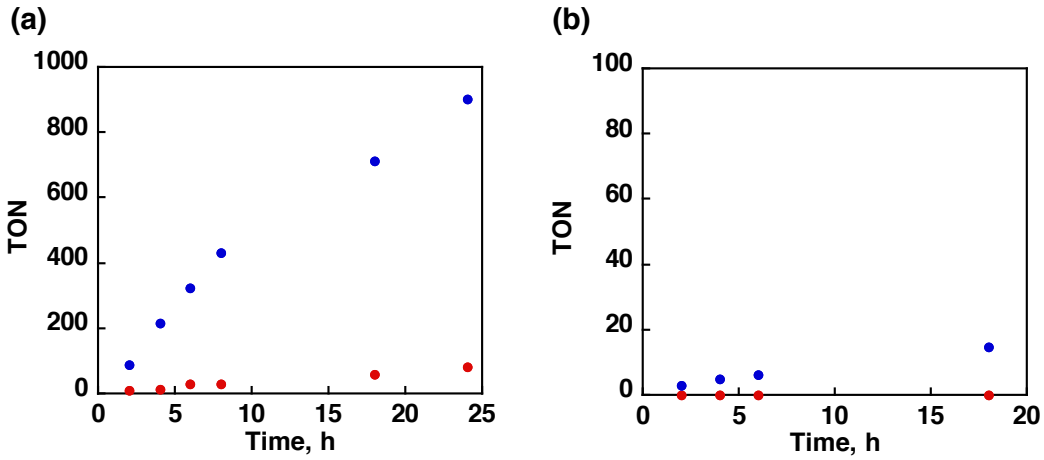

Figure S7. Time profiles of the amount of products [methylphenylsulfoxide (blue) and methylphenylsulfone (red)] for photocatalytic oxidation reaction of thioanisole (2.0×10^{-2} M) by $Mn^{III}(TBP_8Cz)$ (1.0×10^{-5} M) (a) in the presence of HOTf (2.0×10^{-5} M) and (b) in the absence of HOTf under photoirradiation (white light) in an O_2–saturated PhCN at room temperature.

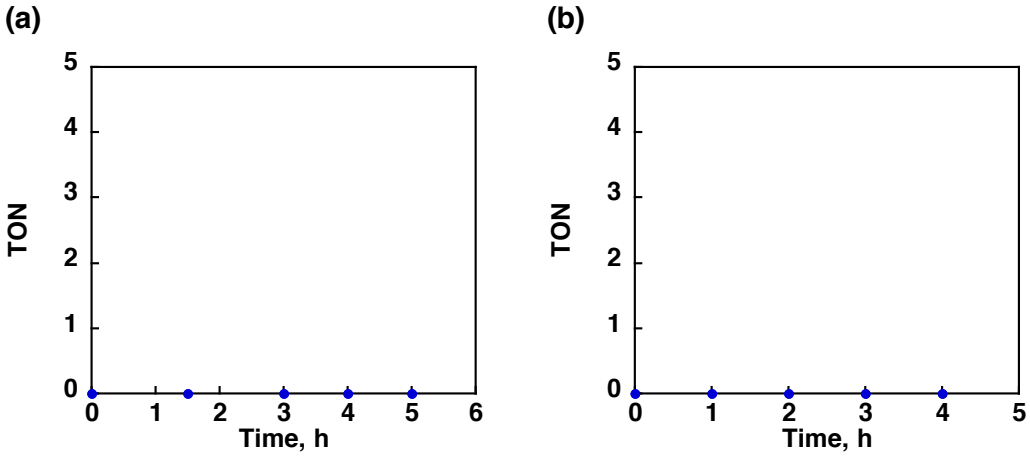

Figure S8. Time profiles of the amount of methylphenylsulfoxide for (a) photocatalytic reaction of thioanisole (2.0×10^{-2} M) in the presence of HOTf (2.0×10^{-5} M) under photoirradiation (white light) in O_2–saturated PhCN at room temperature and (b) the reaction of thioanisole (2.0×10^{-2} M) by $Mn^{III}(TBP_8Cz)$ (1.0×10^{-5} M) in the presence of HOTf (2.0×10^{-5} M) without photoirradiation in O_2–saturated PhCN at room temperature.

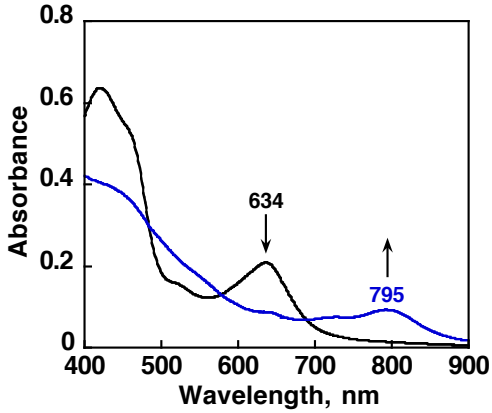

Figure S9. (a) UV-vis spectral changes from $Mn^{V}(O)(TBP_8Cz)$ (black line, 1.0×10^{-5} M) to $[Mn^{IV}(OH)(TBP_8Cz^{\bullet+})](OTf)$ in the presence of HOTf (blue line, 2.0×10^{-4} M) in PhCN at room temperature.

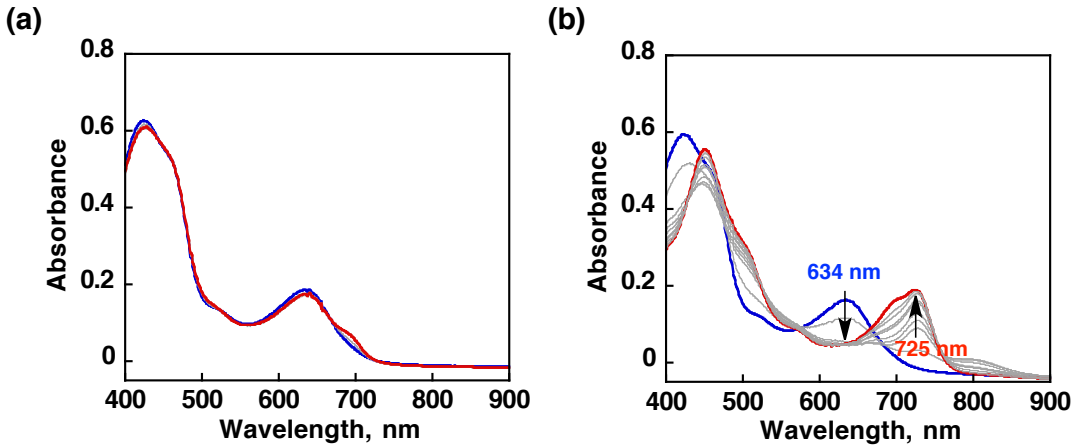

Figure S10. UV-vis spectral changes from $Mn^{V}(O)(TBP_8Cz)$ (blue line, 1.0×10^{-5} M) with HMB (2.0×10^{-2} M) to $Mn^{III}(OTf)(TBP_8Cz(H))$ (red line) (a) in the absence of HOTf and (b) upon addition of HOTf (2.0×10^{-5} M) in a PhCN solution for 1 h at room temperature.

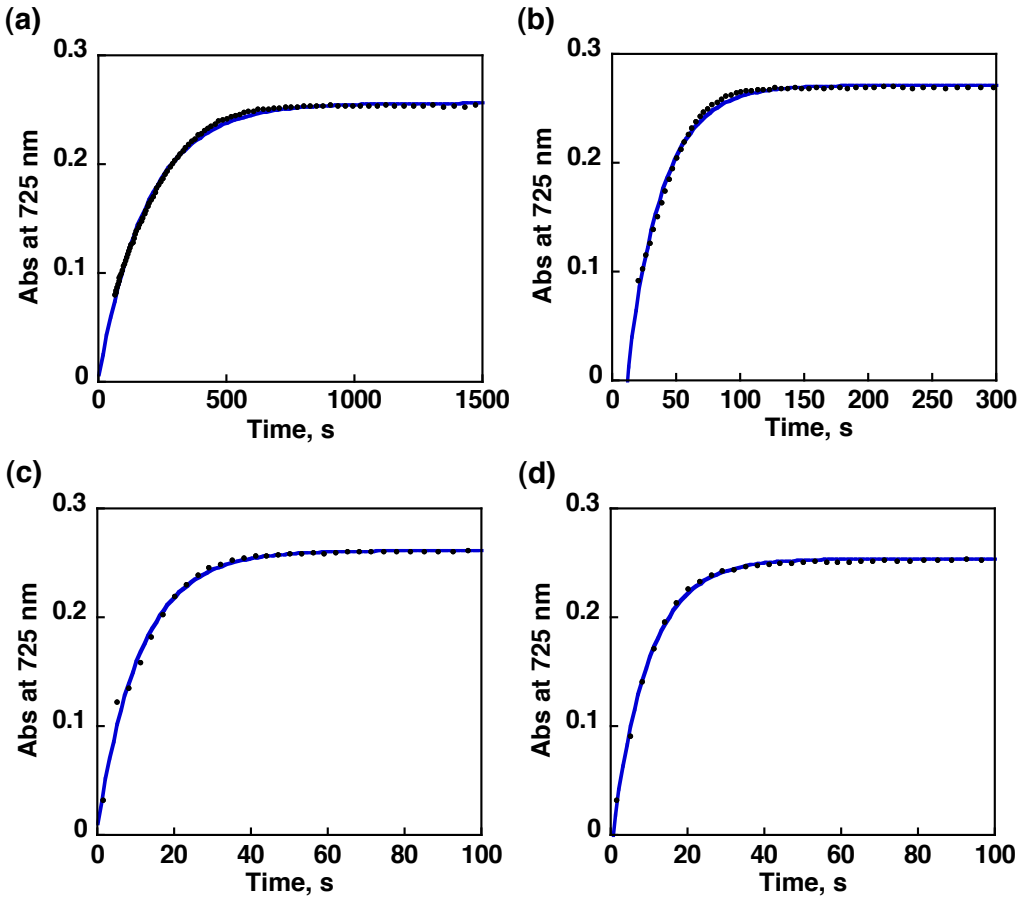

Figure S11. Plots of formed $Mn^{III}(OTf)(TBP_8Cz(H))$ (λ_{max} = 725 nm) versus time and best-fit lines to give pseudo-first-order rate constant (k_{obs}) of the reduction reaction of $[Mn^{IV}(OH)(TBP_8Cz^{\bullet+})](OTf)$ (1.0×10^{-5} M) with HMB (2.0×10^{-2} M) in PhCN containing (a) 20 μM, (b) 40 μM, (c) 80 μM, and (d) 90 μM of HOTf.

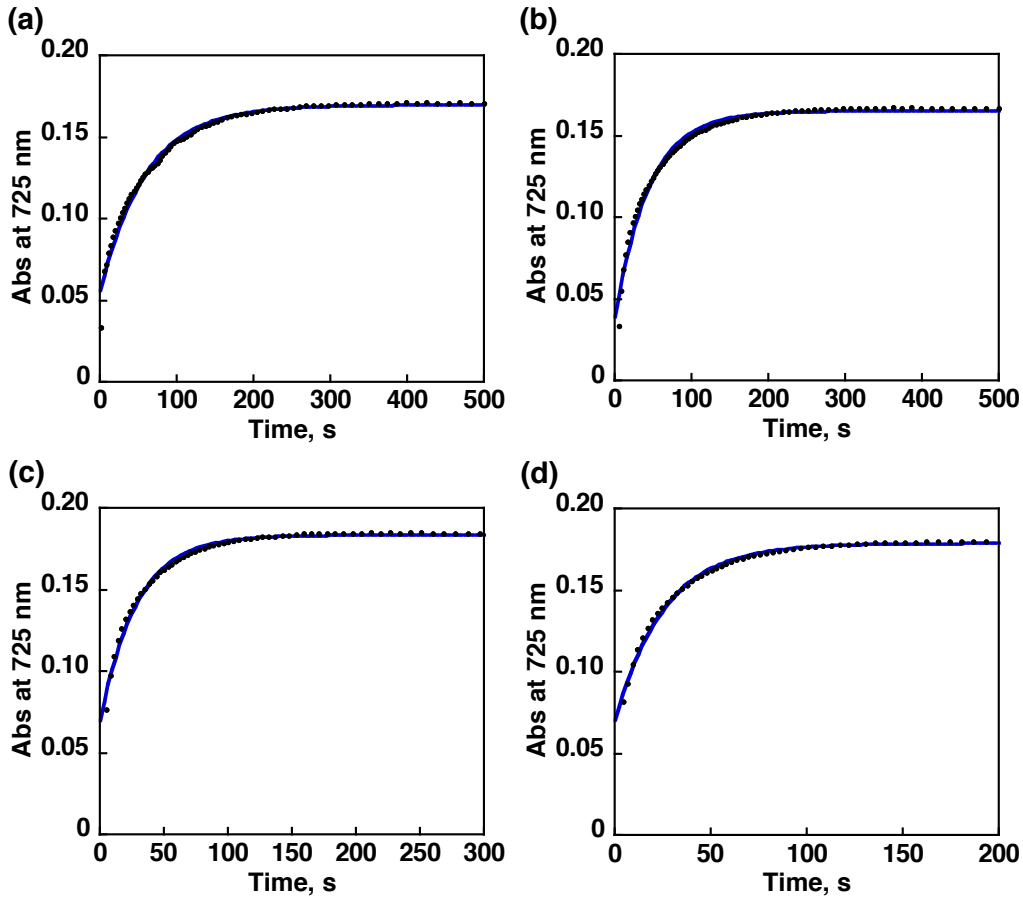

Figure S12. Plots of formed $Mn^{III}(OTf)(TBP_8Cz(H))$ (λ_{max} = 725 nm) versus time and best-fit lines to give pseudo-first-order rate constant (k_{obs}) of the reduction reaction of $[Mn^{IV}(OH)(TBP_8Cz^{\bullet+})](OTf)$ (1.0×10^{-5} M) with HOTf (3.0×10^{-5} M) in PhCN containing (a) 2 mM, (b) 4 mM, (c) 6 mM, and (d) 8 mM of HMB.

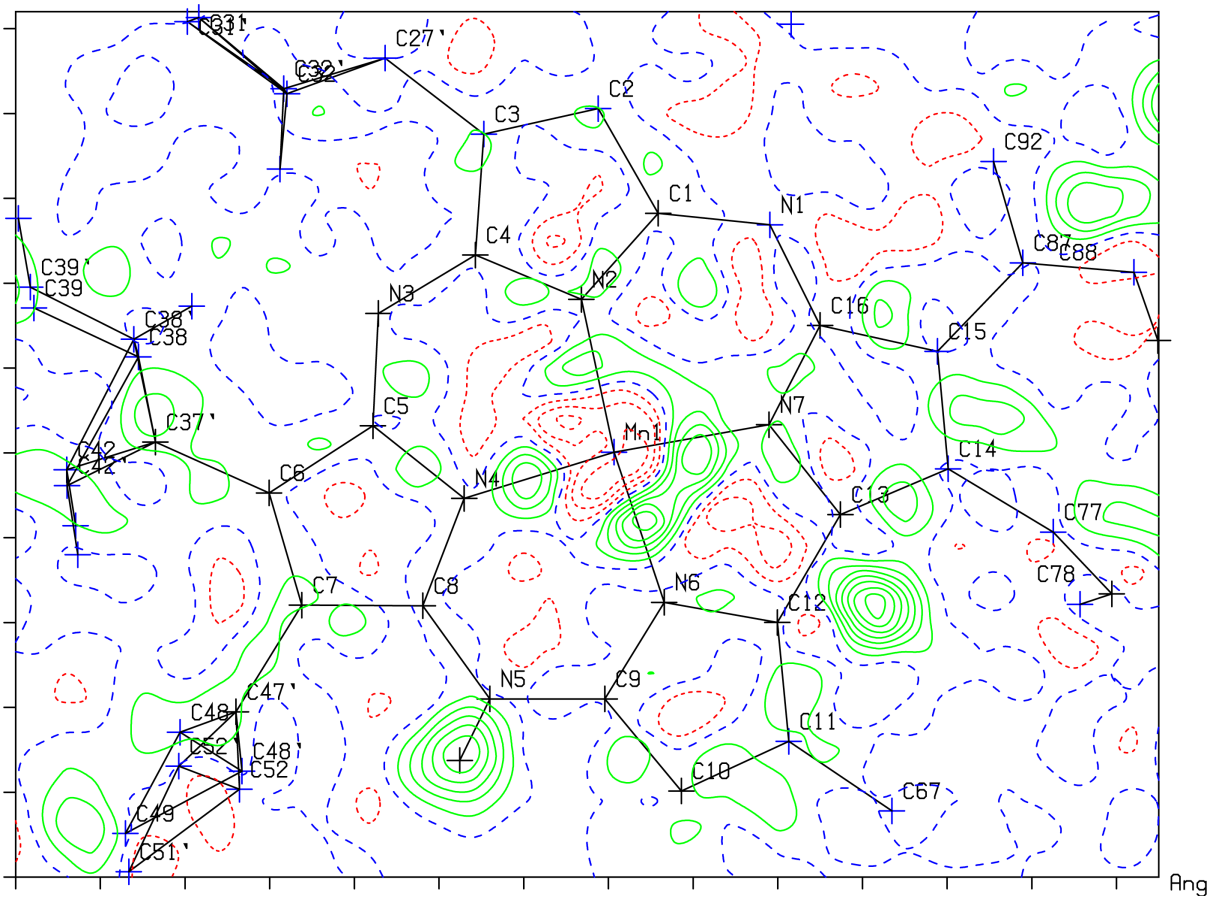

Figure S13. Difference Fourier map of Mn^{III}(OTf)(TBP_8Cz(H)) at 110(2) K drawn on the plane of the corrolazine core. N5 is the identified protonated site.

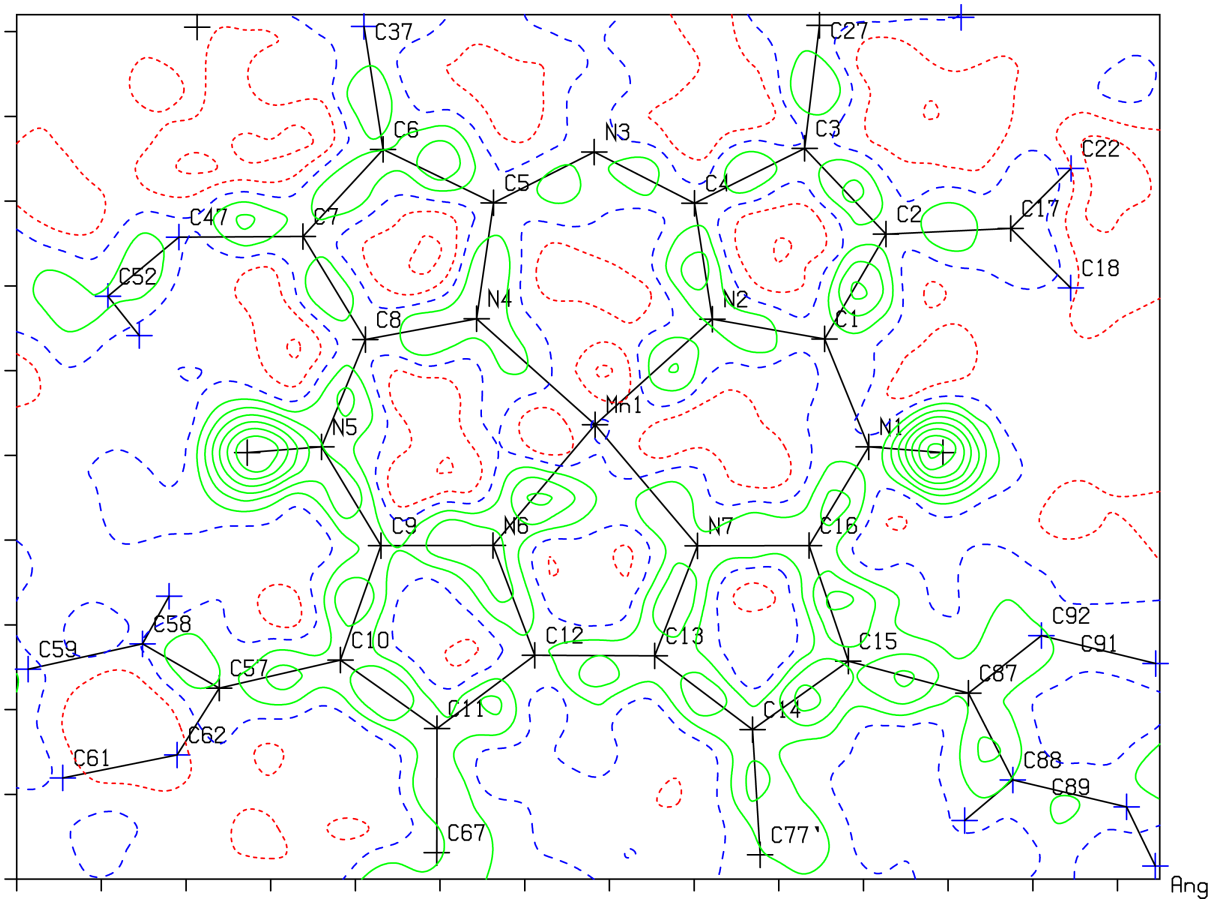

Figure S14. Difference Fourier map of $[Mn^{III}(OTf)(H_2O)(TBP_8Cz(H)_2)][OTf]$ at 110(2) K drawn on the plane of the corrolazine core. N1 and N5 are the identified protonated sites.